SIMULATING QUANTUM PHYSICS BY INTEGRATED PHOTONIC CIRCUITS

LINDA SANSONI[1], NICOLÒ SPAGNOLO[1], CHIARA VITELLI[1,2], FABIO SCIARRINO[1,3], PAOLO MATALONI[1,3]

[1] *Dipartimento di Fisica, Sapienza Università di Roma, Roma, Italy*
[2] *Center for Life NanoScience @ Sapienza, Istituto Italiano di Tecnologia, Roma, Italy*
[3] *Istituto Nazionale di Ottica, Consiglio Nazionale delle Ricerche (INO-CNR), Firenze, Italy*

Modern quantum technologies allow to isolate, manipulate, control, and detect single particles, enabling specific tasks that would be inaccessible to systems operating classically, in particular to reproduce, *i.e.* to simulate, the dynamics of quantum phenomena. However many of these demonstrations are still far from real-world applications. In this perspective, new horizons may be disclosed by recent achievements in quantum simulation experiments performed with quantum photon states. They are based on the use of integrated photonic devices having the potential of speeding-up the evolution from lab systems to the next generation of quantum optical devices for real-world applications.

1 Introduction

Quantum information (QI) originated in the late 80's and early 90's from the merging of classical information and quantum physics. This research field, which has undergone a huge and rapid growth of the last few years, has the potential to revolutionize many areas of science and technology. It is multidisciplinary by nature, with scientists coming from diverse areas, both in theoretical and experimental physics, such as atomic physics, quantum optics and laser physics, condensed matter, up to computer science, mathematics, material science and engineering. The main goal of QI is to manipulate and to process the information by using quantum systems, in particular for the control and manipulation of the degrees of freedom of quantum particles. On this perspective, completely new schemes of information transfer and processing, enabling new forms of communication and enhancing the computational power, are expected to be developed. Indeed, while QI holds the promise of immense computing power, far beyond the capabilities of any classical computer, it guarantees, in principle, absolutely secure communication and it is directly linked to novel quantum technologies and devices.

Quantum Information usually deals with quantum bits, or "qubits", *i.e.* 2-dimensional quantum systems that do not possess in general the definite values of 0 or 1 of classical bits, but rather are in a coherent superposition of the two orthogonal basis states. Such state reveals unusual properties, especially when dealing with composite systems. The most distinctive feature of quantum physics is given by the possibility of entangling different qubits. First recognized by Erwin Schroedinger as "the characteristic trait of quantum mechanics", quantum entanglement represents the key resource for modern QI processing. It derives from subtle non-local correlations between the parts of a quantum system and combines three basic structural elements of quantum theory, namely the superposition principle, the quantum non-separability property and the exponential scaling of the state space with the number of partitions. Quantum entanglement, that has no classical analogue, when associated with non-classical correlations

among separated quantum systems, can be used to perform computational and cryptographic tasks that are impossible with classical systems.

Important research efforts have been focused in the last few years within the QI community on the simulation of quantum physical processes. As first envisaged by Feynman [1], nothing can beat a quantum system in simulating another quantum system. A quantum simulator is indeed a quantum system that can be controlled in its preparation, evolution and measurement and whose dynamics can implement that of the target quantum system we want to simulate. Several examples can be given in this context, for instance the energy transfer within photosynthetic systems, displaying quantum effects such as delocalized excitonic transport, may be simulated by the so-called quantum walk. Moreover, a light-harvesting molecule is well described by the Anderson localization of a quantum walker: the molecule is efficient in concentrating light at its center as quantum walk reaches the target vertex exponentially faster than a classical walk because of destructive interference between the paths pointing backward, towards the leaves. As a final example, the entanglement can be associated to the interaction between spin-1/2 particles in order to mimic the transition from localized valence-bond configuration to the superposition of different valence-bond states, a phenomenon which might explain high-temperature superconductivity in cuprates.

Among the different approaches to QI technologies, quantum optics represents an excellent experimental test bench for a large variety of novel concepts. Photons are in fact the natural candidate for QI transmission since they are practically immune from decoherence and can be distributed over long distances, both in free-space and in low-loss optical fibres. Photons are also important for future quantum networks and represent an obvious choice for optical sensing and metrology, finally they are a promising candidate for computing. Quantum states of photons can be easily and accurately manipulated using both linear and non-linear optical devices and can be efficiently measured by efficient single-photon detectors. In quantum optics the qubit is implemented by a single photon which realizes a quantum state with a discrete number of levels. Efficient single photon and/or entangled photon sources are required. Pairs of entangled photonic qubits are usually generated by the spontaneous parametric down-conversion (SPDC) process in a 2nd-order non-linear crystal where, under suitable conditions, a pump photon of frequency ν_p is annihilated and two photons of frequencies ν_1 and ν_2 are created, with $\nu_p = \nu_1 + \nu_2$, along the wave vectors $\mathbf{k}_1$ and $\mathbf{k}_2$, with $\mathbf{k}_p = \mathbf{k}_1 + \mathbf{k}_2$. Qubits are generally implemented by adopting photon polarization states, with entangled states realized by the orthogonal states corresponding to the horizontal (H) and vertical (V) polarizations. Further examples of photonic qubits are given by other accessible degrees of freedom, such as longitudinal momentum, orbital angular momentum and the conjugated variables of energy and time.

Up to now the implementation of optical systems of up to 8 qubits has provided a large amount of exciting results giving an unprecedented insight in the quantum world. The obtained experimental results range from fundamental tests of quantum mechanics (non-locality tests, quantum contextuality) to quantum computing (implementation of algorithms, simulation of chemical systems) and optical quantum metrology (quantum illumination, quantum imaging and sensing).

Both single-qubit and two-qubit operations need to be addressed with high sensitivity in order to operate efficiently with multi-qubit systems, a requirement which is out of reach with the up to date experimental approaches. It is worth remembering that the current technology does not allow to extend the previous achievements because of many practical limitations. In fact, the development of increasingly complex quantum-optical schemes realized by bulk optics suffers from severe limitations as far as stability, operation precision and physical size are concerned. Using individual bulk-optical components to build just one interferometric structure, providing the stability and the accuracy of the optical phase control required by quantum mechanics, is an extremely difficult task. Furthermore, it is virtually impossible to achieve this task outside environments with controlled temperature and vibration, and this makes any application outside laboratory not achievable.

A recent breakthrough is represented by the emergence of integrated photonic technology in the realm of quantum applications, giving rise to a new generation of integrated waveguide structures consisting of complex quantum circuits with almost perfect intrinsic phase stability [2]. Integrated photonics enables the fabrication of on-chip platforms for powerful applications of quantum communication and computation and allows to solve critical problems in terms of scalability and reliability. Using the mobility of photons we are able to create arbitrary interconnections within interferometer arrays fabricated on single integrated platforms and to realize complex optical circuits performing basic quantum logic gates and algorithms [2-4] and representing the hardware of a quantum simulator operating with photons.

In this article we present the main quantum simulation experiments performed with integrated photonic circuits by our group at Sapienza Università di Roma, in strong synergy with the group of IFN-CNR (Istituto di Fotonica e Nanotecnologie – Consiglio Nazionale delle Ricerche) and Politecnico di Milano.

2 Quantum interference within integrated photonic devices: the beam splitter

Unusual effects may be observed when two or more quantum light beams are combined together; just think, for example, of quantum interference, which arises from the superposition of two coherent light beams. To observe these phenomena, devices able to manipulate light are needed. Among the different devices the most simple one is the so-called "beam splitter" (BS). It is an optical element able to divide a light beam impinging on it (fig. 1a): a photon incoming on a BS is in a superposition state being reflected and transmitted at the BS interface, according to its reflectivity. When dealing with quantum light, this device allows to observe a particular phenomenon with no counterpart in the classical world. Let us consider a BS with 50% reflectivity, and two photons impinging each on the input ports. Since each photon has 50% probability to be reflected or transmitted, on a classical point of view we expect two possible final scenarios: photons emerge both from the same output (one photon is reflected at the BS while the other is transmitted) or they emerge from different outputs (both photons are reflected or transmitted). These events occur with the same probability ½.

When two quantum (*i.e.* indistinguishable) photons are impinging on the BS, a surprising effect arises: due to their bosonic nature, photons always emerge from the same output (fig. 1b left), a phenomenon known as the Hong-Ou-Mandel (HOM) effect [5]. It has no classical analogue, and represents an important resource in many QI research areas, from quantum computation to quantum metrology. This result makes the BS a basic element for quantum experiments with light.

We may ask at this point: how does an entangled state behave on a BS? The answer is simple and quite surprising. In this case we must take into account the symmetry of the wave function. Let us consider as input states for the beam splitter the two-photon entangled states

$$|\xi^{\pm}\rangle = \frac{1}{\sqrt{2}}\left[|2\rangle_1 |0\rangle_2 \pm |0\rangle_1 |2\rangle_2\right] ,$$

where $|n\rangle_j$ represent a state with n photons in the input j. Clearly $|\xi^{+}\rangle$ is symmetric under particle exchange, while $|\xi^{-}\rangle$ is antisymmetric.

It is easy to demonstrate that, when an entangled symmetric state is injected in the BS, the resulting output will be entangled with two photons emerging from the same output mode, while in the opposite case the two photons will emerge always from different outputs (fig. 1b). This result is obtained for a two-photon state entangled in the path (or in the longitudinal momentum **k**) of photons, which is the same degree of freedom the BS acts on, thus, its action can affect the entanglement. In a different manner, if we inject one photon per mode and the two photons share entanglement in other degrees of freedom (*e.g.* polarization, orbital angular momentum, etc.), since the BS acts on the longitudinal momentum, the entanglement in other degrees of freedom will not be affected by its action. Nevertheless, because of symmetric entanglement, photons will emerge

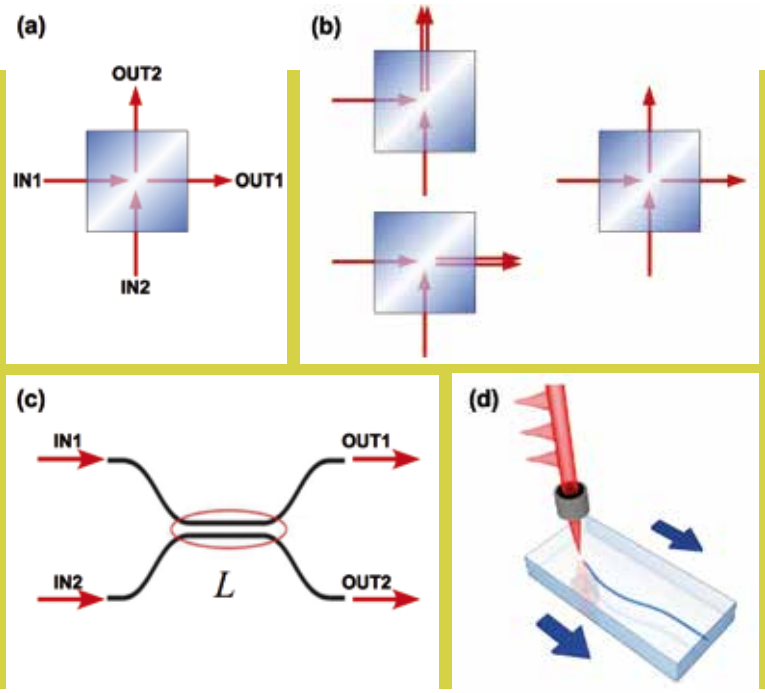

Fig. 1 (a) Scheme of a bulk beam splitter (BS) with input and output modes. (b) Possible output configurations when two photons are injected into the BS: photons emerge from the same output (left) or one per output (right). (c) Scheme of a directional coupler of length *L*, the integrated version of a bulk beam splitter. In analogy with inset (a) input and output ports are shown. (d) Ultrafast laser writing technique: a femtosecond laser is focused on a glass substrate. By moving the substrate with respect to the laser beam it is possible to directly write a waveguide in the bulk of glass.

simultaneously from the same output, while antisymmetric entanglement will result in a state with one photon per output mode. This concept is at the basis of the simulation of fermionic and bosonic statistics performed in our experiment with integrated photonic devices and using polarization entangled photons. We may, thus, observe both the bosonic and the fermionic behavior of two-particle systems with the same physical system (photon pairs), simply exploiting the entanglement between them.

3 Laser written integrated directional coupler

As said, modern communication technology is based on integrated devices: there are many advantages in using integrated devices due to their small dimensions, the intrinsic stability and the potential scalability. Optical waveguides are the basic elements of photonic integrated devices. In this context, the integrated version of the bulk beam splitter is represented by two waveguides arranged in the geometry of a *directional coupler* (DC) whose scheme is depicted in fig. 1c. Provided that the two waveguides are sufficiently close to each other, their fields overlap, hence light can be coupled from one waveguide to the other and the optical power can be transferred between them in a periodic way with light "jumping" back and forth between the two waveguides. This mechanism achieves BS-like operations in integrated photonics and the reflectivity of the integrated BS depends on the length of the interaction region.

Among the various techniques adopted for realizing integrated photonic devices, the use of ultrashort laser pulses for direct writing photonic structures within a glass or a crystal [6] presents peculiar features, in particular:

1. The capability of realizing complex optical circuits in the three dimensions of space;
2. A rapid device prototyping, with the device pattern easily varied by a simple software control;
3. Simpler and less expensive production plants.

We focus on the femtosecond micromachining of bulk transparent materials – *i.e.* materials with no linear absorption at the laser wavelength. When a femtosecond laser pulse is tightly focused within a transparent material energy is deposited in a small volume around the focus due to a combination of multiphoton absorption and avalanche ionization. The glass substrate can be translated along or perpendicular to the beam propagation direction in such a way that waveguides are directly written within the substrate (fig. 1d). In suitable experimental conditions, by taking advantage of its 3-dimensional capability, the ultrafast laser writing technique allows to realize polarization-independent directional couplers, able to transport photons without altering their polarization state. This important feature has been exploited by using polarization-entangled photon states, as described in the following.

4 Entangled photon states within a directional coupler

As a first element for quantum simulation with integrated optics, we used a simple symmetric directional coupler and verified the predicted behavior occurring with polarization-entangled photon pairs.

Ultrafast laser written beam splitters (ULWBS) were

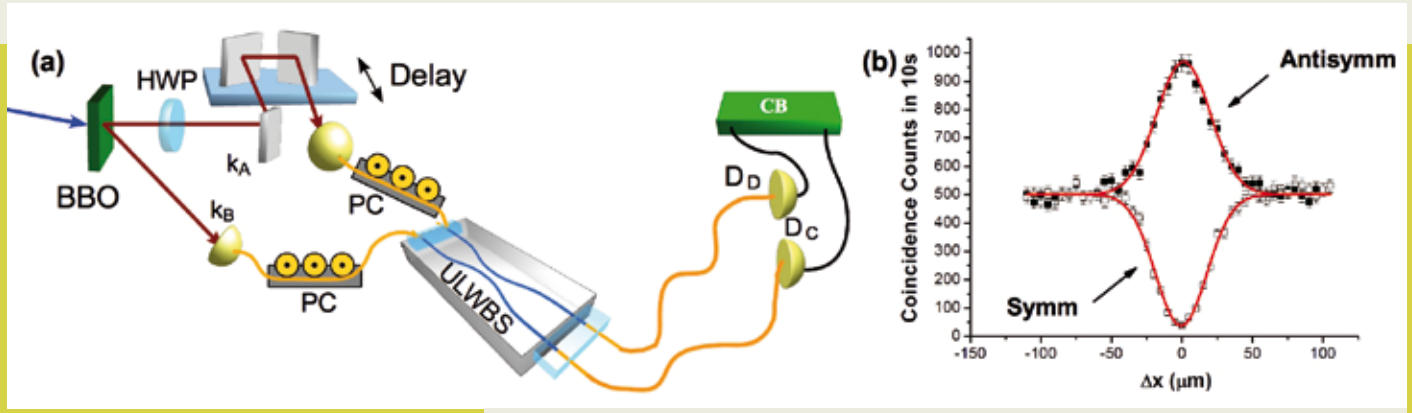

Fig. 2 (a) Setup for two-photon bosonic coalescence on the ultrafast laser written beam splitter: polarization-entangled photon pairs are generated in a β-barium borate (BBO) crystal. A delay line is inserted in one of the two photon paths to vary the temporal delay between the photons. A half waveplate (HWP) allows to switch from symmetric to antisymmetric entanglement. Pairs are delivered through single-mode fibers to the ULWBS and polarization controllers (PC) compensate the rotations induced by the fibers. The outcoming light is detected (D) and coincidences between photons are collected (CB) [8]. (b) Coincidences counts *vs.* photon delay: depending on the input state symmetry we observe a dip or a peak of measured coincidences at zero delay.

fabricated at CNR-Politecnico di Milano with the directional coupler geometry, as shown in fig. 1c. We exploited this device to observe the HOM effect with polarization-entangled states. To this purpose we adopted the experimental setup shown in fig. 2a: polarization-entangled states generated by SPDC [7] were delivered to the ULWBS through single-mode fibers. Photons emerging from the two outputs were revealed by two single-photon counting detectors and detection coincidences between them were recorded. By varying the temporal delay between the two photons arriving at the ULWBS, it is possible to observe the transition from the classical to the quantum behavior, occurring when photons arrive simultaneously. We recorded coincidences between detectors A and B for different temporal delays by injecting both symmetric and antisymmetric entangled states. The results are shown in fig. 2b: when a symmetric state enters the DC, photons emerge always from the same output, thus coincidences between the two detectors vanish for perfect temporal matching, while for an antisymmetric state, photons exit the ULWBS always from different outputs, thus we observe an enhancement in the coincidence counts.

The measured visibility, defined as $V = \left| \frac{C_0 - C_{int}}{C_0} \right|$ where C_0 and C_{int} correspond, respectively, to the coincidence rate outside interference (*i.e.* with spatial delay larger than the photon coherence length) and inside interference (zero spatial delay). The measured visibility is $V_{sym} = 0.929 \pm 0.005$ for symmetric entangled pairs, while it is $V_{ant} = 0.930 \pm 0.005$ in the case of the antisymmetric input state. These results demonstrate the capability of the ULWBS to support the polarization of photons, thus opening the way towards the use of integrated photonics for polarization-encoded qubits [8].

5 Quantum simulation by quantum walks

One of the most promising approaches for quantum simulation tasks is represented by quantum walks (QWs). Quantum walk is an extension of the classical random walk, performed by a walker on a lattice "jumping" between different sites with a given probability. Let us consider a quantum particle – such as an electron, an atom or a photon – on a lattice. As expected the quantum properties of the walker will affect its dynamics. In particular, the peculiar features of the quantum walker, represented by interference and superposition, lead to a non-classical dynamic evolution.

Among the various experimental platforms adopted to implement quantum walks, the optical approach requires single-photon states, beam splitters, phase shifters and single-photon detectors. Let us consider a symmetric discrete walk on a line. Here, each site of the lattice may be implemented by an optical beam splitter (represented by the white boxes in fig. 3a). A photon arriving on one port of the BS is reflected or transmitted with probability $p = 1/2$, thus the walker moves one step right or left along the lattice. A N-step QW may be realized by arranging the BS lines in a cascaded configuration, where each vertical line of beam splitters (fig. 3a) represents a step of the quantum walk.

Once the reflectivity of each BS and the initial position of the walker are given, it is easy to calculate the probability of finding the walker at site j after N steps. The final probability distribution will arise from the interference between all the possible paths the photon may follow along the QW circuit and, at variance with the classical case, where the expected output distribution has its maximum at the central output modes, photons tend to reach the external

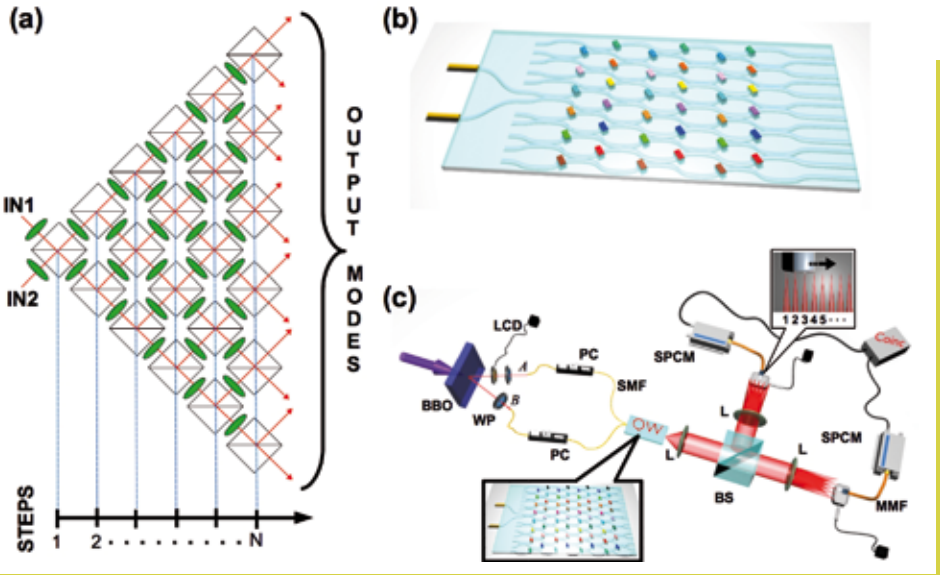

Fig. 3 (a) Photonic implementation of Quantum Walk (QW): an array of cascaded BS (white boxes) and phase shifters (green ovals). (b) Integrated waveguide structure of a QW circuit realized by femtosecond laser writing on a glass. Coloured boxes represent phase shifters. (c) Setup for two-particle QW measurements: polarization entangled photon pairs are generated by spontaneous parametric down-conversion and delivered to the integrated QW circuit (lower inset). The output of the chip is magnified by a set of lenses (L) and divided by a bulk BS. Photons emerging from each output of the QW are detected (upper inset) and coincidences between photons are recorded (Coinc) [10].

sites of the lattice. In such a scenario we may also ask what happens when the walker travels along a QW in the presence of disorder. By introducing disorder, multipath interference is indeed altered and the final distribution will result completely modified depending on the disorder configuration. One might guess that disorder destroys the "quantumness" of the walk, however, surprisingly, this is not the case. Indeed, as predicted by Anderson [9], transport in a medium, in the presence of a position-dependent disorder, leads to a localization of the walker wave function: in this case the particle tends to remain localized instead of wandering along the lattice.

6 Photonic implementation of quantum walks

The QW network depicted in fig. 3a is given by an array of Mach-Zehnder (MZ) interferometers, each one representing the elementary mesh of the network. It is worth stressing that an efficient realization of the BS network is practically impossible to achieve with standard bulk optical components, even for a small number of steps, since it requires a quadratically growing number of elements. Furthermore, a correct operation of the quantum walk strongly requires a controlled and stable phase in each lattice unit mesh. Our approach exploits an integrated waveguide architecture, which allows to concentrate a large number of optical elements within a small chip and to achieve intrinsic phase stability due to its monolithic structure. As said, in our waveguide implementation BSs are replaced by directional couplers realized by the femtosecond laser writing technique. The integrated version of the scheme reported in fig. 3b was given by an array of polarization-independent directional couplers. QW structures of 4, 6 and 8 steps were realized, with each phase of the MZ unit set to zero, enabling in this way a perfect and stable matching of the entire network.

In this context, disorder can be added in the QW evolution by simply introducing (randomly selected) phase shifts (green ovals in fig. 3a) within each MZ unit. Indeed the introduction of a random phase shift corresponds to change the probability for the walker to go left or right at each step. In particular, the time-independent disorder needed to enforce Anderson localization on the photonic walker is obtained in the case of a so-called *static* disorder, *i.e.* by keeping constant the phases for all the MZs corresponding to the same lattice site.

In the experiment each phase shift was obtained during the LW process by slightly lengthening one of the optical path in each MZ interferometer enabled by nanometrical control of the writing process. The experimental investigation of these complex interference effects is enabled by the perfect phase stability provided by miniaturized integrated waveguide circuits. We thus simulated transport in the presence or absence of disorder by using photons travelling along QW circuits realized with the femtosecond laser writing technique, while the entanglement in the polarization degree of freedom, which is not affected by the circuit, was exploited to simulate bosonic and fermionic statistics [10, 11].

7 Quantum walks in ordered structures

The circuit shown in fig. 3b was adopted to implement a discrete one-dimension quantum walk for entangled particles. To carry out and characterize the different quantum walks, we adopted the experimental setup shown in fig. 3c. We prepared polarization entangled two-photon states with symmetric and antisymmetric entanglement and injected them into the integrated QW. Then we measured the coincidences between

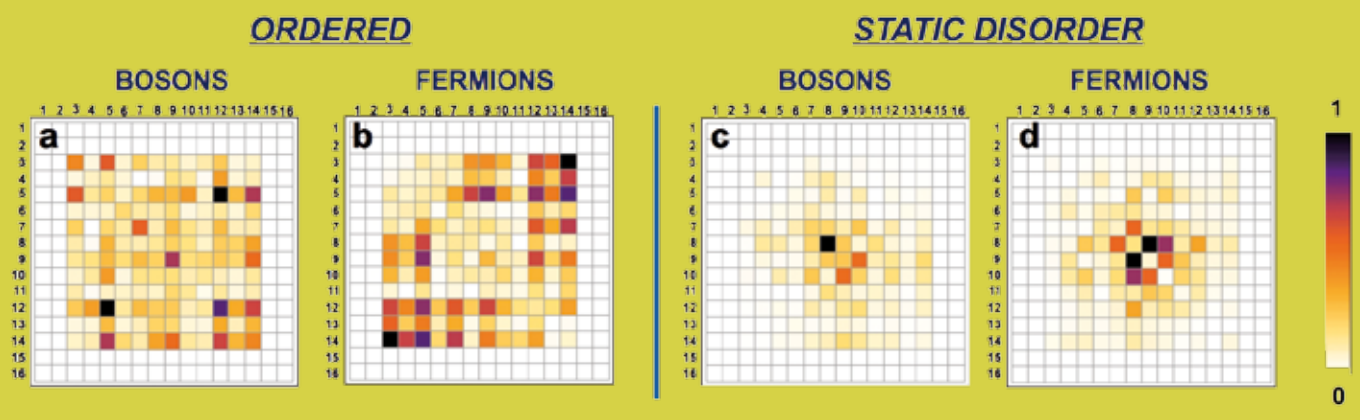

Fig. 4 Bosonic (a, c) and fermionic (b, d) two-particle probability distributions measured on a 8-step QW with ordered structure (a, b) and in the presence of static disorder (c, d) [11]. Each distribution is normalized to its maximum.

all the different outputs, obtaining the corresponding two-particle probability distribution. In figs. 4 a, b we report as an example the bosonic and fermionic distributions for a 8-step QW [10]. It is easy to observe that the distributions spread in the lattice, moreover bosonic and fermionic QWs present a deep difference: due to Pauli exclusion principle, fermions never emerge from the same output mode, thus the diagonal elements of fermionic distributions are vanishing, while, because of the boson bunching effect, non-zero contributions on the principal diagonal are obtained. The diagonal elements of fig. 4b are not perfectly vanishing because of residual imperfections of the glass chip.

8 Quantum walks in the presence of disorder

We experimentally studied the localization properties of a pair of non-interacting particles obeying bosonic/fermionic statistics by simulating a one-dimensional QW of a two-photon polarization-entangled state in a disordered medium. In this case one-dimensional static-disordered QWs were implemented by setting suitable phase maps within the optical lattice.

The same measurements described in the previous section were performed and the two-particle experimental distributions are reported in figs. 4 c, d for a 8-step QW [11]. We observe in this case an evident localization of the wave function, because of the larger probability occurring in the central sites, while it is very low in the external sites of the lattice. We may still observe a difference between bosons and fermions. Since fermions can not emerge from the same site they arrange in the nearest-neighboring sites obeying Pauli exclusion principle, while bosons localize on a single peak on the diagonal.

9 Multiport beam spitters

The possibility of achieving interference of more than two particles on a beam splitter is a further challenging task [12, 13] which could open the door to the observation of quantum phenomena in increasing-size systems and to the engineering of quantum states for QI processing. Multiport beam splitters are a key ingredient to achieve these purposes: they have been proposed to perform additional classes of possible non-locality experiments in a Hilbert space with dimension $d > 2$. Moreover, the applications to quantum interferometry of three- and four-port beam splitters have been theoretically investigated, and the quantum enhancement in terms of sensitivity has been predicted [14]. The behaviour of N photons impinging onto the N-port beam splitter can be studied by a statistical approach, since the complexity of this problem grows faster than exponentially with growing N.

10 Experimental interference of three photons in a tritter

The three-beam extension of a beam splitter, the so-called "tritter" was first addressed in ref. [15] and its proposed implementation consisted in a set of conventional beam splitters and phase shifters (fig. 5a). We realized the first experimental investigation of 3-photon interference in an integrated tritter, realized by femtosecond laser waveguide writing [16] (fig. 5b).

Because of bosonic coalescence, when the tritter is injected by three indistinguishable photons entering the three input ports, all the terms of two photons exiting from the same output port disappear (fig. 5c). In order to fully describe the three-photon interference, we need to introduce two

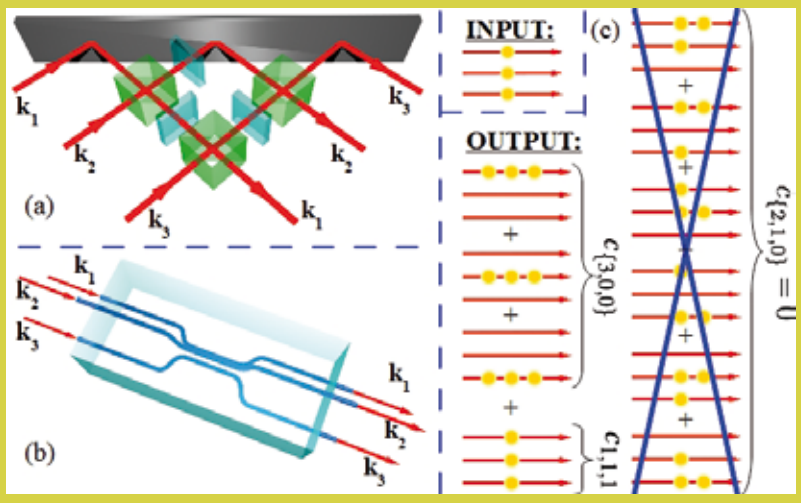

Fig. 5 (a) Optical scheme for a three-mode splitter obtained by a set of conventional beam splitters (grey cubes) and phase shifters (green plates), where $\mathbf{k}_i$, with $i = 1,2,3$ represent input-output spatial modes. (b) Integrated 3-dimensional scheme for a laser-written tritter. (c) Three-photon bosonic coalescence effect in a tritter when each photon is injected into a different input spatial mode. In ideal conditions all the terms with two photons exiting on the same output port vanish due to bosonic coalescence [16].

relative delays between the three particles. We theoretically calculated the probability of the different output states [(1,1,1), (2,1,0), (3,0,0)] as a function of the relative delays $x_m = c\tau_m$ ($m = 1, 2$) between the three photons. These probabilities are represented in figs. 6a-c as surfaces in a 3-dimensional space and represent an extension of the well-known HOM curves. This representation enables a deeper insight into three-photon interference, evidencing non-trivial features as a function of the two delays. In particular, we observe the presence of three regions: i) the three input photons are indistinguishable, this leads to a three-photon coalescence effect, resulting in a dip or a peak depending on the detected output state; ii) only two of the three input photons are indistinguishable; iii) the three input photons are distinguishable, leading to classically correlated outcomes.

The particles, each coupled to a different waveguide, mutually interfere in the three-arm directional coupler by evanescent field interaction. The behaviour of a three-photon state entering the tritter was investigated by comparing the output state probabilities with the expected classical ones, evidencing the purely quantum effects involved in bosonic coalescence.

The three-photon coalescence was tested by adopting the experimental setup shown in fig. 7, using four photons created by two SPDC processes: one of them was acting as the trigger for coincidence detection, while the other three photons were coupled inside the tritter, after passing through different delay lines. The output modes were detected by using optical fiber beam splitters and single-photon counting detectors. Coincidences between different detectors were used to reconstruct, by post selection, the probability of obtaining a given output state. By changing the relative delays between the three photons we could observe the coalescence effects in the different experimental conditions, as shown in fig. 8. Precisely, with a three-photon state injected in the three input ports, we measured the different output contributions, $|1,1,1\rangle$, $|2,1,0\rangle$, $|3,0,0\rangle$.

Due to a partial distinguishability between photons belonging to different pairs, the expected interference visibilities change depending on which photon is delayed. Figure 8 shows the experimental and theoretical output states probabilities, obtained by delaying photons in different input modes for each measured output state. Three-photon interference is reported when delaying the

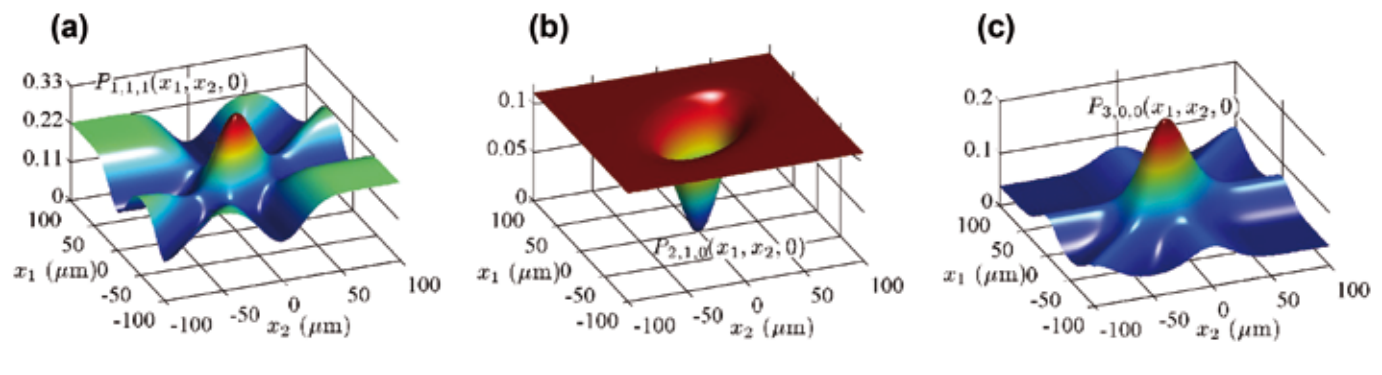

Fig. 6 Hong-Ou-Mandel effect for a $|1,1,1\rangle$ input state in an ideal tritter. Theoretical output probabilities $P_{1,1,1}$ (a), $P_{2,1,0}$ (b), and $P_{3,0,0}$ (c) as a function of the delays $x_i = c\tau_i$ of the impinging photons [16].

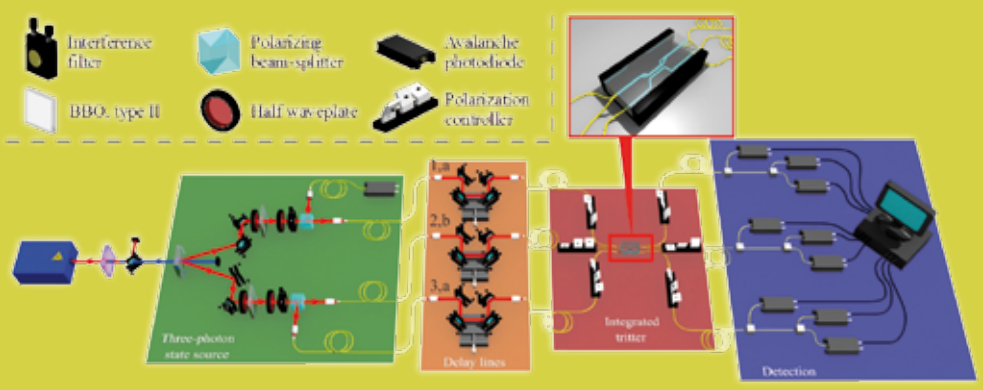

Fig. 7 Experimental setup for the characterization of the tritter and the three-photon coalescence experiment. Two-photon and three-photon states, generated by SPDC, are injected in the tritter device after the propagation through spatial delay lines. Then, coincidence detection at the output ports is performed to reconstruct the probability of obtaining a given output state realization (i, j, k). Labels 1, 2, 3 stand for spatial modes, while letter *a* refers to indistinguishable photons and *b* to the partially distinguishable one. BBO represents β-barium borate crystal [16].

partially distinguishable photon (case A in the figure) or when delaying one of the two indistinguishable ones (case B in the figure). In addition, we also considered the case when the partially distinguishable photon was kept out of the interference region and properly delaying the two indistinguishable ones (case C in the figure). The latter case corresponds to the standard two-photon interference. It is observed that cases A and B are clearly different from case C. This demonstrates that the output states that we observe in cases A and B are indeed due to three-photon interference and cannot be attributed to two-photon interaction. By comparing the obtained visibilities with the classical bounds, calculated by injecting the tritter with three equal-amplitude coherent states with randomized phases, we found that the results obtained with the input state outperform classical predictions, thus demonstrating the quantum origin of the measured three-photon interference.

Multiport directional couplers, as the symmetric tritter, have the potential to become fundamental elements for future complex networks implemented by integrated optical circuits. Indeed, these devices may find a wide range of applications in both quantum interferometry and quantum metrology. Recent theoretical analysis indicate that they can be exploited to build *N*-mode interferometers where the adoption of quantum input states can lead to a significant enhancement in phase estimation protocols. Furthermore, the capability of conditionally generating path-entangled states may be increased by adopting structures composed of *N*-port beam splitters rather than conventional two-mode couplers. Several other contexts may benefit from the adoption of *N*-port beam splitters. For instance, they can be adopted for the realization of "proof-of-principle" quantum simulators, and, combined in a modular structure, they can be used to realize full-scale quantum simulators for large size quantum systems.

11 The problem of BosonSampling

The fascinating, long-term goal of a quantum computer promises a large computational advantage in solving problems which are otherwise intractable with classical computers [3]. However, despite the strong experimental effort and the recent advances in the quantum information field, the realization of a large-scale quantum computer is still far from the current state of the art. It is then crucial to identify possible intermediate steps showing an evidence of the computational advantage of quantum systems. This includes for instance systems whose evolution cannot be predicted with classical computers, but with a reduced number of resources with respect to a large-scale quantum computer.

Recently, it has been shown by Aaronson and Arkhipov [17] that bosonic particles and linear unitary transformations are a promising candidate for an intermediate milestone showing the potential of quantum systems. Indeed, the evolution of a system of bosons undergoing arbitrary linear unitary transformations, a task known as BosonSampling (fig. 9a), rapidly becomes hard to predict using classical computers as we increase the number of particles and modes. The hardness of the task derives from the relationship between the

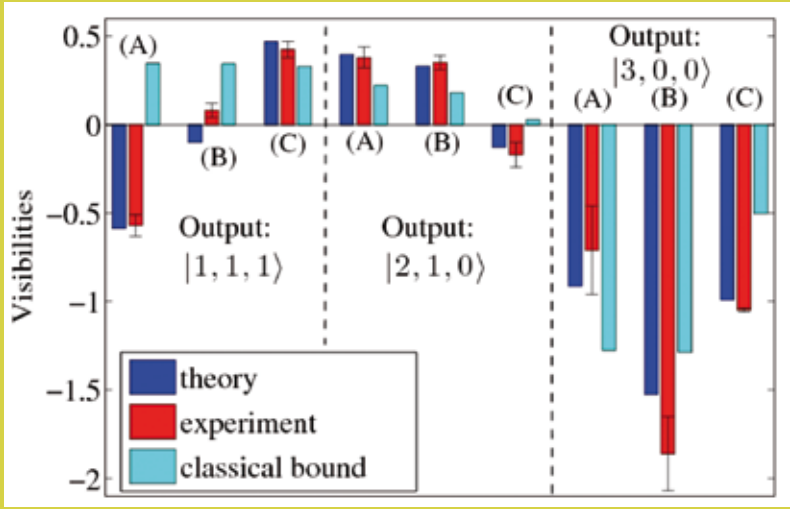

Fig. 8 Visibility measured for different choices of the delayed photon and of the measured output state contribution. Case A: distinguishable photon on input port 2 delayed (three-photon interference). Case B: identical photon on input port 3 delayed (three-photon interference). Case C: distinguishable photon on input port 2 out of the interference region and identical photon on input port 3 delayed (two-photon interference). Blue bars: theoretical prediction obtained from the reconstructed tritter matrix and partially distinguishable photon pairs. Red bars: experimental results. Cyan bars: expected visibilities with classical states. Error bars are due to Poissonian statistics of the measured signal [16].

transition amplitudes of the process and the permanent of square matrices. Aaronson and Arkhipov estimated [17] that a system of approximately 20 particles in a linear network of 400 modes would take a sufficiently long time to be predicted with a classical computer. This behavior of bosonic particles, such as photons, is in contrast with the fermionic case, whose evolution can be easily calculated with a classical computer because of the relationship existing in this case between the transition amplitudes of the process and the determinant of the corresponding matrix.

A natural platform to solve the BosonSampling is provided by photons evolving through linear optical interferometers. This suggests a feasible experiment to demonstrate the computational capabilities of quantum systems, consisting essentially of observing the multi-photon interference of Fock states in a sufficiently large multimode linear optical interferometer. This theoretical result, combined with recent developments in the field of integrated photonics, motivated a strong experimental effort in this direction to obtain the first demonstration of small instance of the BosonSampling problem. This has lead recently to four simultaneous parallel experiments reported by different international collaborations [18-21].

A generic *m*-mode interferometer, described by an arbitrary unitary matrix, can be in principle implemented by using only standard passive linear optical elements. More specifically, it consists of a network of directional couplers with different transmittivities (in the range [0,1]) and intermediate phase-shifters (in the range [0,π]). The architecture for the case $m = 5$ is shown in fig. 9b. As shown in previous sections, the fabrication of such structures may be provided by adopting integrated femtosecond laser-written waveguides. In the present implementation of the BosonSampling problem we considered the realization of a randomly chosen interferometer. Indeed, for specific choices of the system under investigation, symmetry arguments can be exploited to reduce the computational complexity of the network. In order to implement any possible unitary transformation, it is necessary to build integrated interferometers with independent control of both beam splitter transmittivities and phase shifters, as shown in fig. 9c. As already seen, phase shifters are implemented by deforming the waveguides at the input of each directional coupler in order to modify the optical path. The 3-dimensional capabilities of femtosecond laser-writing were exploited to modify the beam splitter transmittivities without changing the path lengths (and hence without introducing additional undesired phases). This is achieved by rotating one arm of the directional coupler out of the main circuit plane, thus modifying the transmission between paths.

In the experiment we generated three single photons by two simultaneous SPDC photon pair processes and injected them in the *m*-mode interferometer (fig. 10a), then we proceeded as follows. First, we picked randomly a 5-mode interferometer, evaluated the values of fabrication parameters (beam splitters and phase shifters), and then realized the corresponding integrated device. It is then crucial to check that the actual device resembles closely the desired interferometer. To this end, we performed a tomographic characterization of the unitary matrix which describes the action of the device without assuming any *a priori* knowledge of the system. This task can be achieved

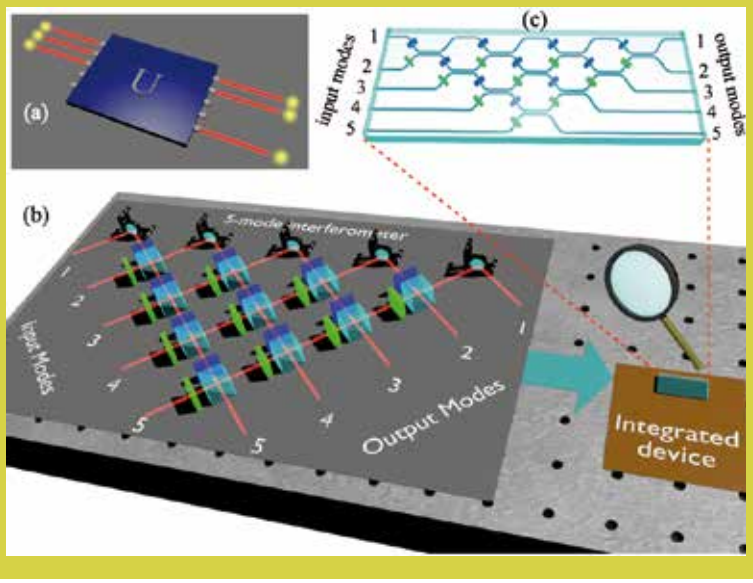

Fig. 9 (a) The concept of BosonSampling: the distribution of *m* bosons is reconstructed after evolution through a linear transformation. (b) Architecture for an arbitrary 5-mode interferometer, composed by beam splitters (cyan cubes) and phase shifters (blue and green boxes). (c) Corresponding architecture for an arbitrary integrated 5-mode device.

by probing the device with both single-photon and two-photon states. More specifically, we measured the probability that a single photon injected in input port *i* exits from output port *k*. Conversely, the two-photon measurements were done by simultaneously injecting two single photons on all ten combinations of two different input modes (*i, j*). Then, for each input state, we measured all possible HOM interference patterns on output ports (*k, l*) by introducing a time delay between the two photons. This set of measurements corresponds to 25 single-photon probabilities and 100 two-photon interference experiments, and is sufficient to fully reconstruct the action of the implemented interferometer.

The results of the single-photon and of the two-photon measurements are shown in figs. 10 b, c and compared with the corresponding predictions obtained from the reconstructed unitary matrix. The agreement between two distributions p_k and q_k is quantified by the distance $d = 1/2\sum_k |p_k - q_k|$, which ranges in the interval [0, 1] where the 0 value is obtained when the two distributions are identical. The average distance between the predictions of the reconstructed matrix and the experimental data, averaged over the values corresponding to all the different inputs, is $d^1_{exp'r} = 0.065 \pm 0.003$ (single photon experiments) and $d^2_{exp'r} = 0.103 \pm 0.013$ (two-photon experiments), which indicates a good quality in the characterization process. The quality of the fabrication process is confirmed by the distance between the experimental data and the predictions of the ideal matrix, given by $d^1_{exp't} = 0.158 \pm 0.003$ and $d^2_{exp't} = 0.221 \pm 0.013$. This small distance provides a confirmation of the proper functioning of the device.

The second step corresponds to testing multimode interference in the multiphoton regime. More specifically, we injected the three photons in the input ports (1,3,5), and we measured the probability ratios of how the three photons distribute among the different output ports. We then compared the measured results with the predictions obtained by calculating with the permanent formula the output distribution expected from the reconstructed unitary matrix. The results of the three-photon measurements are shown in fig. 10d. A good agreement between the predicted distributions and our experimental results is obtained, as quantified by the distance between these two distributions $d^3_{exp'rt} = 0.105 \pm 0.024$. These results provide an experimental confirmation of the permanent formula in the three-photon, five-mode regime.

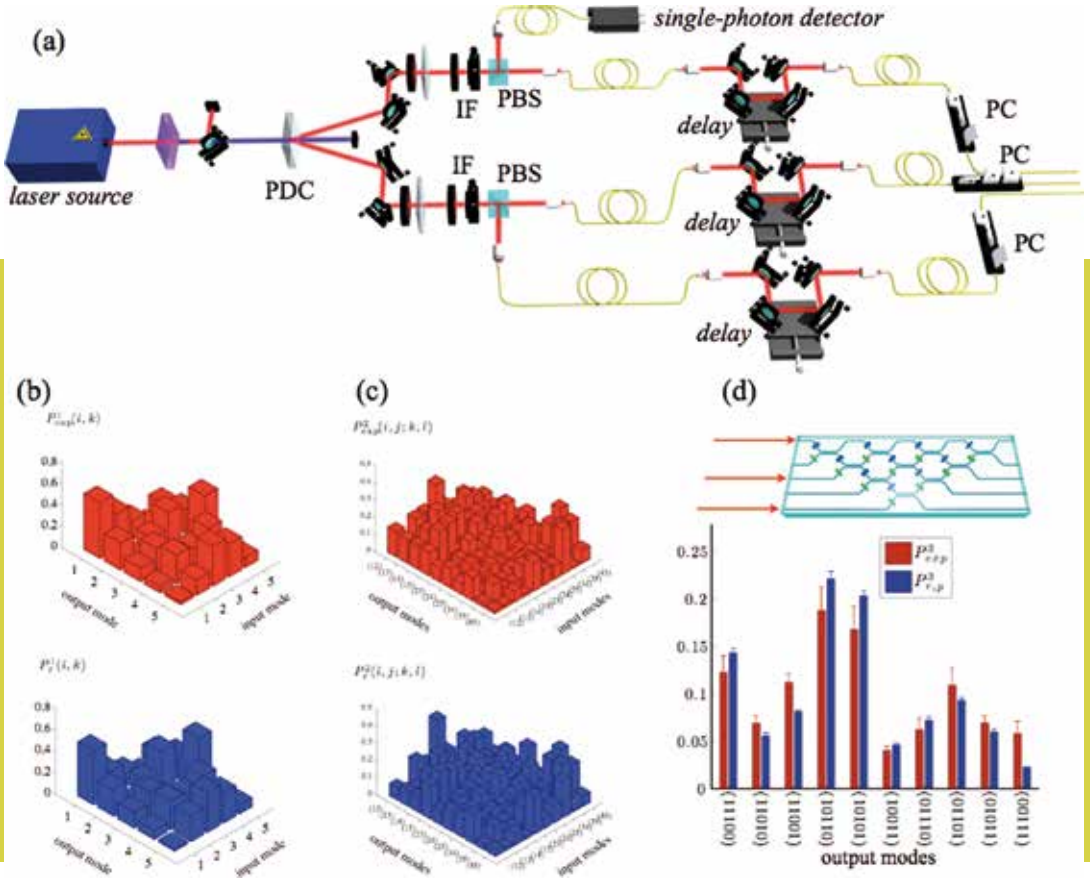

Fig. 10 (a) Experimental setup for the generation of single-, two- and three-photon states. Photons are generated through the process of parametric down-conversion (PDC). After spectral selection by interference filters (IF), polarization selection through polarizing beam splitters (PBS), coupling into single-mode fibers and polarization compensation (PC), they are injected in the integrated interferometer. (b) Single-photon, (c) two-photon and (d) three-photon measurements (red bars) compared with the predictions obtained with the permanent formula from the reconstructed unitary matrix (blue bars) [21].

12 Conclusions

Quantum information science has found great experimental success with the implementation of quantum photon states. To date, however, the majority of quantum optical experiments use large-scale (bulk) optical elements bolted down to an optical bench; an approach that ultimately limits the complexity and stability of quantum circuits required for quantum science and technology. The realization of complex optical schemes consisting of a large number of elements requires the introduction of waveguide technology to achieve the desired scalability, stability and miniaturization of the device. Integrated waveguide photonic devices are expected to have a large impact in photonic quantum technologies and to achieve a level of complexity larger than what previously demonstrated. Fast reconfigurable waveguide circuits will enable the realization of a variety of integration demonstrators with applications in different scientific and technological areas.

In this paper we have presented some recent experiments carried out with integrated photonic quantum circuits realized within the bulk of glasses by the ultrafast laser writing technique. The capability of this technique to design 3-dimensional circuits in a chip has been exploited to realize complex optical systems and interferometric arrays of beam splitters showing accurate phase and balancement control. The quantum simulation of paradigmatic physical effects in a single chip has been demonstrated. Important perspectives are envisaged towards the future realization of even more complex quantum processors able to overcome the classical boundary for specific classes of problems.

Acknowledgements

The experiments described in this paper have been supported by FIRB-Futuro in Ricerca HYTEQ (Hybrid technologies for quantum information processing), PRIN 2009 (Progetti di Ricerca di Interesse Nazionale 2009), the ERC-Starting Grant 3D-QUEST (3D-Quantum Integrated Optical Simulation; grant agreement no. 307783): `http://www.3dquest.eu.`, QWAD (Quantum Waveguides Applications & Developments), EU-Project CHISTERA-QUASAR (Quantum State Analysis and Realization).

References

[1] R. P. Feynman, *Int. J. Theor. Phys*., 21 (1982) 467.
[2] A. Politi, M. J. Cryan, J. G. Rarity, S. Yu and J. L. O'Brien, *Science*, 320 (2008) 646.
[3] A. Politi, J. C. F. Matthews and J. L. O'Brien, *Science,* 325 (2009) 1221.
[4] A. Crespi, R. Ramponi, R. Osellame, L. Sansoni, I. Bongioanni, F. Sciarrino, G. Vallone and P. Mataloni, *Nat. Commun.,* 2 (2011) 566.
[5] C. K. Hong, Z. Ou and L. Mandel, *Phys. Rev. Lett.,* 59 (1987) 2044.
[6] G. Della Valle, R. Osellame and P. Laporta, *J. Opt. A: Pure Appl. Opt*., 11 (2009) 013001.
[7] P. Kwiat *et al*., *Phys. Rev. Lett.,* 75 (1995) 4337.
[8] L. Sansoni, F. Sciarrino, G. Vallone, P. Mataloni, A. Crespi, R. Ramponi and R. Osellame, *Phys. Rev. Lett*., 105 (2010) 200503.
[9] P. Anderson, *Phys. Rev.*, 109 (1958) 1492.
[10] L. Sansoni, F. Sciarrino, G. Vallone, P. Mataloni, A. Crespi, R. Ramponi and R. Osellame, *Phys. Rev. Lett*., 108 (2012) 010502.
[11] A. Crespi, R. Osellame, R. Ramponi, V. Giovannetti, R. Fazio, L. Sansoni, F. De Nicola, F. Sciarrino and P. Mataloni, *Nat. Photon.*, 7 (2013) 322.
[12] D. M. Greenberger, M. A. Horne and A. Zeilinger, *Phys. Today,* 46, no. 8 (1993) 22.
[13] M. Zukowski, A. Zeilinger and M. A. Horne, *Phys. Rev. A,* 55 (1997) 2564.
[14] N. Spagnolo, L. Aparo, C. Vitelli, A. Crespi, R. Ramponi, R. Osellame, P. Mataloni and F. Sciarrino, *Sci. Rep.,* 2 (2012) 862.
[15] R. A. Campos, *Phys. Rev*., A 62 (2000) 013809.
[16] N. Spagnolo, C. Vitelli, L. Aparo, P. Mataloni, F. Sciarrino, A. Crespi, R. Ramponi and R. Osellame, *Nat. Commun*., 4 (2013) 1606.
[17] S. Aaronson and A. Arkhipov, in *Proceedings of the 43rd Annual ACM Symposium on Theory of Computing* (*ACM Press*) (2011) 333.
[18] M. A. Broome, A. Fedrizzi, S. Rahimi-Keshari, J. Dove, S. Aaronson, T. C. Ralph and A. G. White, *Science* 339 (2012) 794.
[19] J. B. Spring, B. J. Metcalf, P. C. Humphreys, W. S. Kolthammer, X.-M. Jin, M. Barbieri, A. Datta, N. Thomas-Peter, N. K. Langford, D. Kundys, J. C. Gates, B. J. Smith, P. G. R. Smith and I. A. Walmsley, *Science*, 339 (2012) 798.
[20] M. Tillmann, B. Dakić, R. Heilmann, S. Nolte, A. Szameit and P. Walther, *Nat. Photon.*, 7 (2013) 540.
[21] A. Crespi, R. Osellame, R. Ramponi, D. J. Brod, E. F. Galvão, N. Spagnolo, C. Vitelli, E. Maiorino, P. Mataloni and F. Sciarrino, *Nat. Photon.,* 7 (2013) 545.

Paolo Mataloni

Paolo Mataloni is Full Professor at Sapienza Università di Roma where he teaches Optics and Laboratory, and Nonlinear and Quantum Optics. During his career he has worked on the study of phenomena related to the electromagnetic field confinement, such as spontaneous and stimulated emission and superradiance within planar optical microcavities and microlasers. In the last 10 years he has carried out a number of experiments of Quantum Information, dealing with the generation of entangled photon states by spontaneous parametric down-conversion, detection and characterization of entanglement, creation of generalized mixed entangled photon states with tunable mixing parameter, quantum non-locality, besides multiqubit hyperentangled and cluster photon states and their application for quantum computation. More recently he has performed experiments dealing with integrated waveguide photonic systems opening novel perspectives for the experimental simulation of quantum physical processes.